In: Polymers, Polymer Blends, Polymer Composites… ISBN 1-60021-168-2
Eds: A.K. Mikitaev, M.K. Ligidov et al., pp.31-37

Chapter 4

THE ROLE OF DIFFUSIVE PROCESSES IN MODEL REACTION OF REETHERIFICATION

Lyubov Kh. Naphadzokova** and Georgi V. Kozlov
Kabardino-Balkarian State University, Nal'chik, Russian Federation

ABSTRACT

It is shown, that the offered model of diffusive processes for chemical reactions describes well the main characteristics of model reaction of reetherification. A structure of reaction product (heptylbenzoate molecule) and forming parts of it are the main factor controlling diffusive processes in this case. Mentioned processes are described within the framework of strange (anomalous) diffusion.

Keywords: Chemical reaction, reetherification, scaling, fractional differentiation, active time, strange diffusion.

INTRODUCTION

One of the perspective ways of search of effective inorganic filler-catalysis's for complex polyethers is kinetic study of the reetherification model reaction, performed in the presence of various inorganic compounds [1]. Such method allows to use obtained results in the synthesis process of filled complex polyethers [2].

Synthesis processes in common case can be considered as the complex system self-organization, developing during time, that results to formation of time-dependent fractal structures [3]. In such reactions the important role is played by diffusive processes, which in the considered case have very specific nature. This specificity is due to the fact, that in chemical reactions not all reagents contacts occur with proper for reaction's product

*Correspondence to: Lyubov Kh. Naphadzokova, Kabardino-Balkarian State University, Nal'chik, Russian Federation, Chernyshevski 173, 360004, mailto: lnaph@freemail.ru

formation orientation of reacting molecules. This aspect of reaction is accounted for by steric factor p ($p \leq 1$) [4]. Variation p can result to the change of diffusion type, structure, reaction's product and, as the consequence, to the rate of chemical reaction change. This question can be explained by a simple example. As it is known [5], characteristic size $r(t)$ of region, which can be visited by the reagent molecule during time t, is equal to:

$$r(t) \sim t^{1/(2+\theta)} \tag{1}$$

where θ is connectivity index of reactive medium.

For the case of classical Gaussian diffusion θ=0 and, believing $r(t)$=2 and t=4 relative units, the equality within the framework of the relationship (1) will be obtained. Such equality assumes p=1, i.e., each contact of reagents molecules results to reaction product formation. Let's assume, that the value p decreases up to 0.05, i.e., only one from 20 contacts of reagents molecules is formed a new chemical sort. This means the increase t in 20 times and then at $r(t)$=2 and t=80 relative units from the relationship (1) will be obtained θ=4.33. Since θ is connected with dimension of walk trajectory of reagents molecules d_w by the simple equation [5]:

$$d_w = 2 + \theta \tag{2}$$

then θ increase results to d_w raising, i.e., is slows down the chemical interactions process.

In its turn, the value d_w is connected with Herst exponent H by the equation [5]:

$$d_w = \frac{1}{H} \tag{3}$$

The change θ from 0 up to 4.33 results to raising d_w from 2 (Brownian motion) up to d_w=6.33 according to the equation (2) and to reduction H from 0.5 up to 0.158 according to the equation (3). As it is known [5] subdiffusive (slow) transport processes correspond to the values $0 \leq H < 0.5$ and classical Gaussian diffusion – H=0.5. Therefore, the decrease p from 1.0 up to 0.05 results to qualitative change of diffusion type too: it changes from Gaussian classical to anomalous (strang). Let's note, that the mentioned transition can occur without changing of general diffusive processes in reactive medium, too since it is due to "rejection" of all diffusive phenomena's, not resulting to the chemical reaction, i.e., to formation of new chemical substance. Proceeding from the said above, the purpose of the present paper is to study diffusive processes influence within the framework of the offered treatment on main characteristics of reetherification model reaction.

EXPERIMENTAL

The reetherification model reaction kinetics of methylbenzoate by heptanole-1 in mica presence was studied at 443 K. Mica catalytic activity was determined on the observed rate

constant of first order k_1 at the twentieth multiple of heptanole-1 excess and mica contents 30 mass. % in calculation on the methylbenzoate [2].

The reetherification kinetics was studied on the gas chromatograph "Biokhrom" with using as internal standard diphenyloxide according to the earlier described method [1]. The rate constant k_1 was calculated according to the equation of irreversible reaction of the first order.

The mica flagopit with polydispersity 0.749 and average probable particles size 0.23×10^{-6} m is used. The initial mica (conditional designation NMM) and also mica chemically modified by sodium hydroxide (SMM) and sulphur acid (AMM) were applied.

RESULTS AND DISCUSSION

Earlier it was shown [6], that for reaction of type

$$A + B \rightarrow inert \quad product \tag{4}$$

the scaling relationship is true:

$$\rho_A \sim t^{D/4} \tag{5}$$

where ρ_A is concentration "surviving" in the reaction process particles, t is reaction duration, D is dimension controlling the reaction elapsion.

In case of reaction elapsion in the Euclidean spaces the value D is equal to dimension of this space d and for fractal spaces D is accepted equal to spectral dimension d_s [6]. By graphing $\rho_A=(1-Q)$ (where Q is conversion degree) as a function of t in double logarithmic coordinates the value D from the slope of these graphs can be determined. It was found, that the mentioned graphs fall apart on two linear parts: at $t<100$ min with small slope and at $t>100$ min the slope essentially increases. In this case the value d_s varies within the limits 0.069-3.06. Since the considered reactions are elapsed in Euclidean space, that is pointed by a linearity of kinetic curves Q-t, this means, that the reetherification reaction elapses in specific medium with Euclidean dimension d, but with connectivity degree, characterized by spectral dimension d_s, typical for fractal spaces [5].

The authors [5] have formulated fractional equation of transport processes, having the following form:

$$\frac{\partial^{\alpha}\psi}{\partial t^{\alpha}} = \frac{\partial^{2\beta}}{\partial r^{2\beta}}\left(B\psi\right) \tag{6}$$

where $\psi=\psi(t, r)$ is distribution function of particles, $\partial^{2\beta}/\partial r^{2\beta}$ is Laplacian operator in d – dimensional Euclidean space and B is relation of transport generalized coefficient and d. The introduction of fractional derivatives $\partial^{\alpha}/\partial t^{\alpha}$ and $\partial^{2\beta}/\partial r^{2\beta}$ allows to account for the effects of memory (α) and nonlocality (β) in context of common mathematical formalism [5].

The introduction of fractional derivative $\partial^{\alpha}/\partial t^{\alpha}$ in the kinetic equation (6) allows for random walks in fractal time (RWFT) – "time component" of strange dynamical processes in turbulent mediums [5]. The distinctive feature of RWFT serves the absence of any noticeable jumps in particles behaviour; in this case root-mean-square displacement $\langle r^2(t)\rangle$ increases with t as t^{α}. The parameter α has sense of fractal dimension of "active" time, in which real walks of particles look as random process; interval of active time is proportional to t^{α} [5].

In its turn, the exponent 2β in the equation (6) allows for instantaneous jumps of particles (Levy "flights") from one region to another. Therefore, exponent's relation α/β gives relation of RWFT contact frequencies and Levy "flights". The value β in the first approximation can be adopted as constant and then relation α/β will be inversed proportional to waiting time of chemical reaction realization. The value α/β is equal to [5]:

$$\frac{\alpha}{\beta} = \frac{d_s}{d} \tag{7}$$

In Fig. 1 the dependence Q on α/β for boundary times of the mentioned above parts of dependences ln(1-Q)-ln t (t=60 and 300 min) is shown. As can be seen, linear correlation $Q(\alpha/\beta)$, passing through coordinates origin and assuming raising Q at increase α, is obtained. Therefore, the larger active time t^{α} the more intensively reaction elapses, that, in general has been exputed.

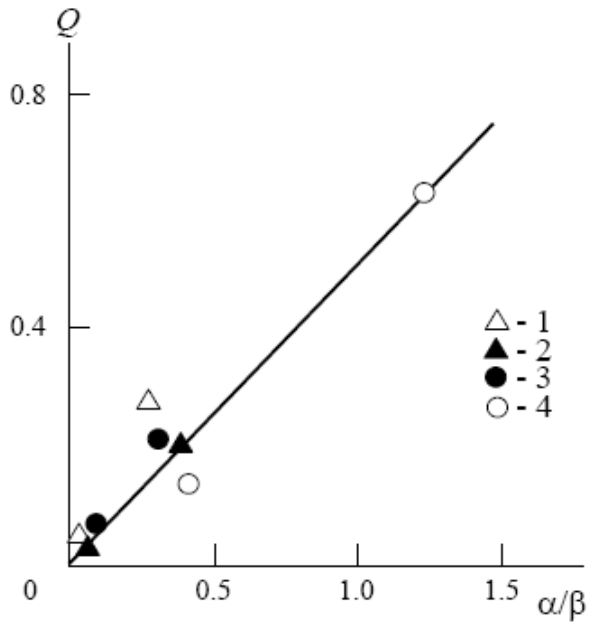

Figure 1. The dependence of conversion degree Q at t=60 and 300 min on relation of the equation (6) exponents α/β for reetherification reaction without mica (1) and in presence of NMM (2), SMM (3), AMM (4)

Next we'll be consider the influence on diffusive processes in the course of chemical reaction of the steric factor *p*, the value of which can be estimated according to the equation (at *t*=10600 s) [7]:

$$p = \frac{1.6}{10600^{(D_f-1)/2}} \tag{8}$$

where D_f is dimension of reetherification product (molecule of heptylbenzoate), determined with the aid of the equation [8]:

$$t^{(D_f-1)/2} = \frac{C_1}{k_1(1-Q)} \tag{9}$$

where C_1 is constant, determined according to the boundary conditions and adopted in present paper equal to 8×10^{-4} s^{-1}.

In Fig. 2 the dependence $\mu^{1/2}=(\alpha/\beta)^{1/2}$ on *p* (such form of correlation was chosen with the purpose of its linearization) is shown. As can be seen, correlation $(\alpha/\beta)^{1/2}(p)$ is actually linear and passes through the origin of coordinates. These points, that, as has been assumed above, diffusive processes in the course of reetherification reaction are controlled by the probability of new chemical substance formation, i.e., molecule of heptylbenzoate.

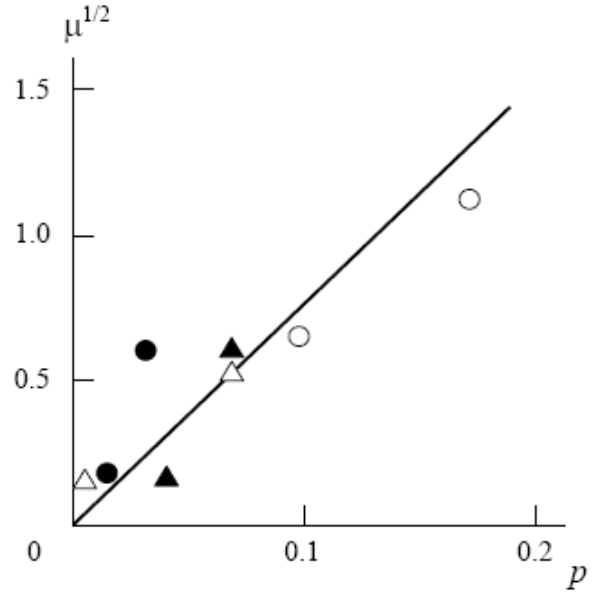

Figure 2. The dependence of the exponent μ on steric factor *p* for reetherification reaction. The notation is the same, as in a Fig. 1

Since $\mu=2H$ [5], then according to the equation (3) can be calculated the value d_w or, more strictly, effective value d_w. In Fig. 3 the dependence $d_w(p)$ is shown, which has very nonlinear form, conditionally dividing into three parts. For small $p<0.025$ large values $d_w \approx 10$-60 are obtained and, correspondingly, large values $D_f \approx 2.13$. This value D_f corresponds to chemically-limited mechanism of cluster-cluster aggregation ($D_f=2.11$), which is characterized by small probability of clusters sticking together or, in other words, by small values p [9]. At $p=0.025$-0.10 the interval $d_w=2$-10 and value D_f reduces in average up to 1.71, that corresponds to diffusive-limited mechanism of cluster-cluster aggregation ($D_f=1.75$) [9]. And at last, the decrease d_w smaller than 2, i.e., the approach of particle trajectories to linear with $d_w=1$, results to formation of heptylbenzoate molecule with $D_f<1.5$. This value D_f corresponds to transparent macromolecular coil dimension [10], i.e., at such dimension molecules of reagents can freely pass through each other, that noticeably facilitates the elapsion of reetherification reaction.

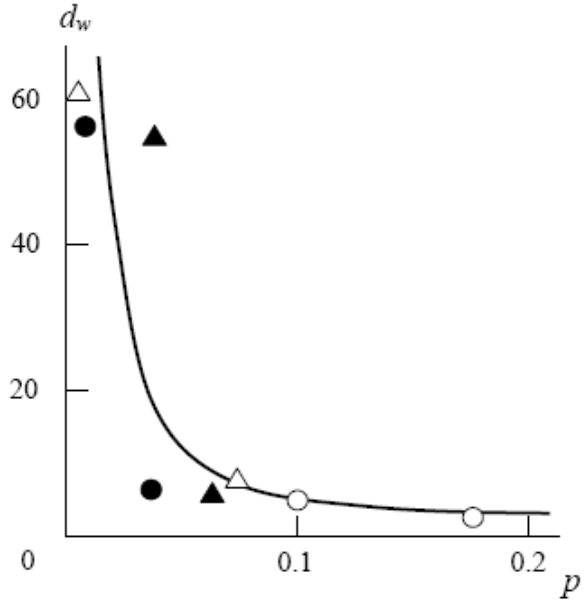

Figure 3. The dependence of walk trajectory of reagents particles d_w on steric factor p for reetherification reaction. The notation is the same, as in a Fig. 1

CONCLUSION

Thus, the results of the present work showed, that the offered model of diffusive processes for chemical reactions describes well the main characteristics of model reaction of reetherification. A structure of reaction product (heptylbenzoate molecule) and forming parts of it is the main factor controlling diffusive processes in this case. Mentioned processes are described within the framework of strange (anomalous) diffusion.

REFERENCES

[1] Naphadzokova, L.Kh., Vasnev, V.A., Tarasov, A.I., *Plast. massy*, 3: 39 (2001).
[2] Vasnev, V.A., Naphadzokova, L.Kh., Tarasov, A.I., Vinogradova, S.V., Lependina, O.L., *Vysokomolek. Soed. A*, 42: 2065 (2000).
[3] Karmanov, A.P., Matveev, D.V., Monakov, Yu.B., *Doklady AN*, 380: 635 (2001).
[4] Barns, F.S., *Biophysica*, 41: 790 (1996).
[5] Zelenyi, L.M., Milovanov, A.V., *Uspekhi Fisichesk. Nauk*, 174: 809 (2004).
[6] Meakin, P., Stanley, H.E., *J. Phys. A*, 17: L173 (1984).
[7] Kozlov, G.V., Shustov, G.B., *in "Uspehki v Oblasti Fiziko-Khimii Polimerov"*. Moscow, Khimia, 2004, 341 p.
[8] Kozlov, G.V., Bejev, A.A., Lipatov, Yu.S., *J. Appl. Polymer Sci.*, 92: 2558 (2004).
[9] Smirnov, B.M., *Uspekhi Fisichesk. Nauk*, 149: 177 (1986).
[10] Baranov, V.G., Frenkel', S.Ya., Brestkin, Yu.V., *Doklady AN SSSR*, 290: 369 (1986).

In: Polymers, Polymer Blends, Polymer Composites… ISBN 1-60021-168-2
Eds: A.K. Mikitaev, M.K. Ligidov et al., pp.39-58

Chapter 5

THERMAL DEGRADATION AND COMBUSTION OF POLYPROPYLENE NANOCOMPOSITE

S. M. Lomakin[1]*, I. L. Dubnikova[2], S. M. Berezina[2], G. E. Zaikov[1], R. Kozlowski[3], Gyeong-Man Kim[4] and G. H. Michler[4]

[1]N.M. Emanuel Institute of Biochemical Physics of Russian Academy of Sciences, 119991 Kosygin 4, Moscow, Russia

[2]N.N. Semenov Institute of Chemical Physics of Russian 119991 Kosygin 4, Moscow, Russia

[3]Institute of Natural Fibres, Poznan, ul. Wojska Polskiego 71 b, Poland

[4]Martin-Luther-Universität Halle-Wittenberg, Geusaer Straße, D-06217 Merseburg, Germany

ABSTRACT

Polypropylene (PP) has wide acceptance for use in many application areas. However, low thermal resistance complicates its general practice. The new approach in thermal stabilization of PP is based on the synthesis of PP nanocomposites. This paper discusses new advances in the study of the thermo-oxidative degradation of PP nanocomposite. The observed results are interpreted by a proposed kinetic model, and the predominant role of the one-dimensional diffusion type reaction. According to the kinetic analysis, PP nanocomposites had superior thermal and fireproof behavior compared with neat PP. Evidently, the mechanism of nanocomposite flame retardancy is based on shielding role of high-performance carbonaceous-silicate char which insulates the underlying polymeric material and slows down the mass loss rate of decomposition products.

Keywords: charring; diffusion; flammability; kinetics; nanocomposite; polypropylene; thermal degradation

*Correspondence to: Sergei M. Lomakin, N.M. Emanuel Institute of Biochemical Physics ofRussian Academy of Sciences, Moscow, Russia, Kosygin 4, 119991, mailto:lomakin@sky.chph.ras.ru

INTRODUCTION

Polypropylene (PP) has wide acceptance for use in many application areas. However, low thermal and flame resistance complicates its general practice.

Much interest has been devoted to the study of PP thermal degradation [1-5]. Earlier studies on the thermal breakdown of polypropylene and its mechanism have been reviewed by Bockhorn et al [1]. The thermal depolymerization of polypropylene was considered as a radical process, which includes initiation, propagation and termination, which is analogous to the mechanism of polyethylene degradation [1]. After the bond scission into primary and secondary radicals, tertiary radicals are formed *via* rearrangements reactions. Subsequent β-scission leads to volatile alkenes and the chain carriers [1]. A β-scission to the other side leads to a short secondary radical and a polymer chain with a terminated double bond. This short secondary radical is saturated *via* intramolecular hydrogen transfer and results in an alkane. Due to the low alkane concentration, transfer reactions seem to play a minor role in polypropylene degradation. The apparent kinetic parameters for the overall thermal degradation of PP were determined under isothermal conditions using a gradient free reactor with on-line mass spectrometry [1]. For pure PP, different investigators have reported values of activation energy from 220–270 kJ/mol [1-3].

Chan and Balke applied thermogravimetric data for the pyrolysis of PP to provide a kinetic model of thermal degradation [4]. However, the wide temperature range used in this work (45–580°C) encompassed a change in the decomposition mechanism and this greatly limited the utility of the methods. To accommodate this mechanism change, the data were treated as a pseudo first-order reaction [4]. It was observed that the data conformed to a first-order fit at temperatures of less than 404 to 421°C (depending upon heating rate) with activation energy of 98.3 ± 3.1 kJ/mol [4]. At higher temperatures the data could again be fit as a pseudo first-order reaction, but with an activation energy of 327.9 ± 8.6 kJ/mol. The two regions were separated by a relatively narrow transition region. The lower activation energy occurring at lower degradation temperatures is attributed to scission of ‘weak links’ in the polymer. The higher activation energy was similar to the carbon-carbon bond dissociation energy and is associated with random scission throughout the polymer [4].

In contrast with many previous publications, Gao et al. showed that a first-order reaction model cannot be applied to describe thermal degradation of polypropylene [5]. The appropriate reaction order was determined to be 0.35 by using the degree of conversion at the maximum degradation rate measured under dynamic conditions. The validity of the reaction order thus determined was verified by similarity of activation energy between the single heating rate plot and the isoconversional plot. The reaction order was also supported by the consistency of the Arrhenius parameters of isothermal degradation with dynamic degradation [5].

The new approach in thermal stabilization of PP is based on polymer nanotechnology [6, 7]. Over the past decade, polymer nanocomposites have received considerable interest as an effective way for developing new composite materials, and they have been studied widely. Because of the larger surface area and surface energy of the additives when individual particles become smaller, it is not an easy task to obtain homogeneously dispersed organic / inorganic composites when the additives are down sized to nano-scale [8]. Melt intercalation has been successful in preparing polymer clay nanocomposites [9].

Recently the thermal degradation behavior of nanocomposites based upon PP-organoclay was studied by Zanetti, Camino *et. al.* using isothermal and dynamic thermogravimetry [10]. They suggested that the oxygen charring action and scavenging effect in the nanocomposite increases as the volatilization proceeds and that in the nanocomposite a catalytic role is played by the intimate polymer-silicate contact that may further favor the oxidative dehydrogenation-crosslinking-charring process.

This silicate morphology may act as an efficient barrier to oxygen diffusion towards the bulk of the polymer. Surface polymer molecules trapped within the silicate are thus brought to a close contact with oxygen to produce the thermally and oxidative stable charred material providing a new char-layered silicate nanocomposite acting as an effective surface shield [10]. In the present study a routine set of TGA analytical data was accomplished to provide the kinetic analysis of thermal degradation in air of PP nanocomposite based on layered organoclay (Cloisite 20A). The results obtained in this study gave an additional evidence of diffusion-controlled character of thermal degradation of PP nanocomposite caused by the catalytic-charring effect of nanosilicate clay.

Lately Qin at al. reported data on polypropylene/montmorillonite (PP/MMT) microcomposites thermal degradation and flammability [11]. They mentioned that PP microcomposites exhibit higher thermal stability and considerably reduced peak heat release rate due to physico-chemical adsorption of the volatile degradation products on the silicates [11]. On the other hand, the addition of MMT can catalyze the initial decomposition of PP matrix and accelerate its ignition in combustion. It has been observed that a ceramic-like char formed on the surface of the composites during the combustion test. The characterization of the char surface prior to ignition indicates that it is an inorganic-rich surface, leading to improvement of the thermal stability and reduction of flammability of the composites because of its better barrier properties [11].

EXPERIMENTAL

Synthesis

Polypropylene (PP) by Moscow petroleum refinery (MFI = 0.7) and maleic anhydride-modified oligomer (MAPP - Licomont AR 504 by Clariant co.) with M_n~2900; MA-content~4 wt.%. were blended/mixed using a laboratory Brabender mixing chamber for 2 min. at the first stage. The concentration of MAPP was 20% by weight of original PP. Then the 7% wt. of organoclay (Cloisite 20A - Na^+ montmorillonite modified by dimethyl, dihydrogenatedtallow ammonium chloride by Southern Clay Co.) was added to the PP-MAPP - melt at a rotor speed of 60 rpm and set temperature of 190°C (PP-MAPP- Cloisite 20A). 10 min. mixing time was used in all the experiments.

Characterization

WAXS analysis of nanocomposite layered structure was carried out with a DRON-2 X-ray Diffractometer with Cu-Kα radiation. Diffraction patterns were collected in reflection-mode geometry from 2° to 10°2θ.

AFM studies were performed with commercial scanning probe microscope Nanoscope IIIA and IV MultiMode (Digital Instruments/Veeco Metrology Group, USA) in tapping mode, at ambient conditions. Conventional etched Si probes (stiffness ~40 N/m, resonant frequency 160-170 kHz) were used. The amplitude of the free-oscillating probe, A_0, was varied in the 10-20 nm range while the set-point amplitude, A_{sp}, ranged from 0.5 to 0.8 A_0. Imaging was conducted on the flat sample surfaces being prepared at –80°C with an ultramicrotome MS-01 (MicroStar Inc., USA) equipped with a diamond knife.

The thermal decomposition studies were performed over a temperature range of 20-600^{o}C using a MOM Q 1500 thermogravimetric analysis (TGA) system under air environment at the scan rates of 3, 5 and 10K/min.

Kinetic analysis of PP compositions thermal degradation was carried out using Thermokinetics software by NETZSCH-Gerätebau GmbH.

RESULTS AND DISCUSSION

Structure Characterization

It is always necessary to carefully characterize the polymer structure in order to ensure a sort of the dispersion for the nanoclays in polymers. XRD analysis and TEM would provide some information on the nanocomposite structural morphology. The diffraction patterns for nanoclay and nanocomposites are displayed in Figure 1 (a). The Cloisite 20A itself has a single peak at around 3.6^o with d-space of 2.4 nm.

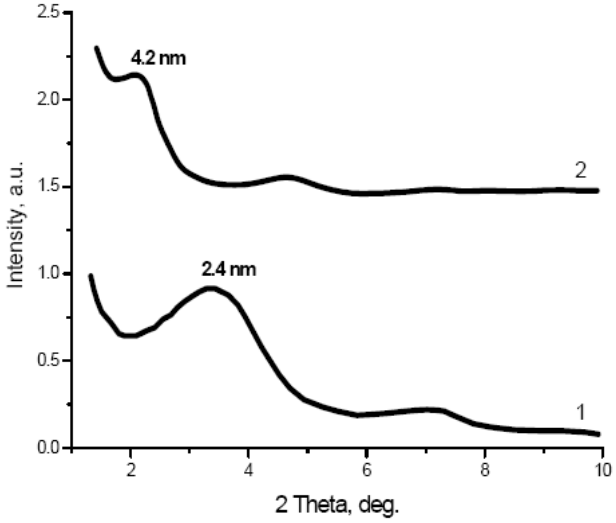

Figure 1. WAXS analysis for Cloisite 20A (1) and PP-MAPP-Cloisite 20A (2)

The shift of the clay basal spacing d_{001} from 3.6° to 2.2° in PP-MAPP-Cloisite 20A sample suggests the intercalated nanocomposite sample have higher d-space (4.2 nm) than that in the original clay (2.4 nm), it may have some exfoliated structures considering the smearing of peak in nanocomposite sample.

However, the XRD can only detect the periodically stacked montmorillonite layers (A); for all these nanocomposites there also exists a small number of exfoliated layers (B) as well, which can be directly observed by transmission electron microscopy (TEM).

In Figure 2 we present TEM images with different magnification which designate the presence of intercalated tactoids (A) and apparently exfoliated monolayers (B) coexisting in the nanocomposite structure. The intercalated structures are characterized by a parallel registry that gives rise to the XRD reflection of Fig. 1.

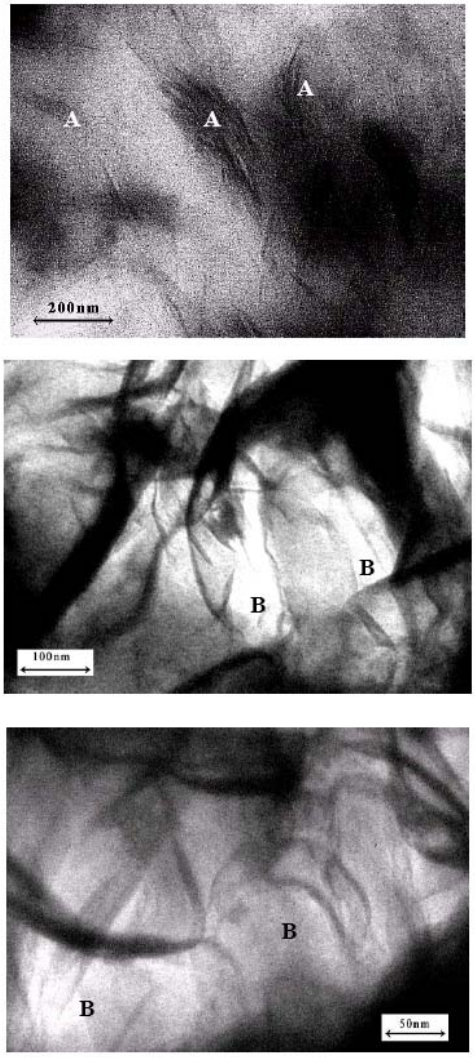

Figure 2.TEM photos with different magnification of PP-MAPP-Cloisite 20A where: A - stacks of layers (intercalated tactoids), B - exfoliated monolayers

AFM studies demonstrate the similar morphology characteristics for PP-MAPP-Cloisite 20A (Fig. 3). Height and phase images were simultaneously recorded on polymer surfaces. Height image presents surface topography, whereas phase images provide a sharp contrast of fine structural features and emphasize differences in sample components. We presume the availability of essentially intercalated structure with the complex multilayered tactoids (A) and small amount of exfoliated monolayer units (B) (Fig. 3).

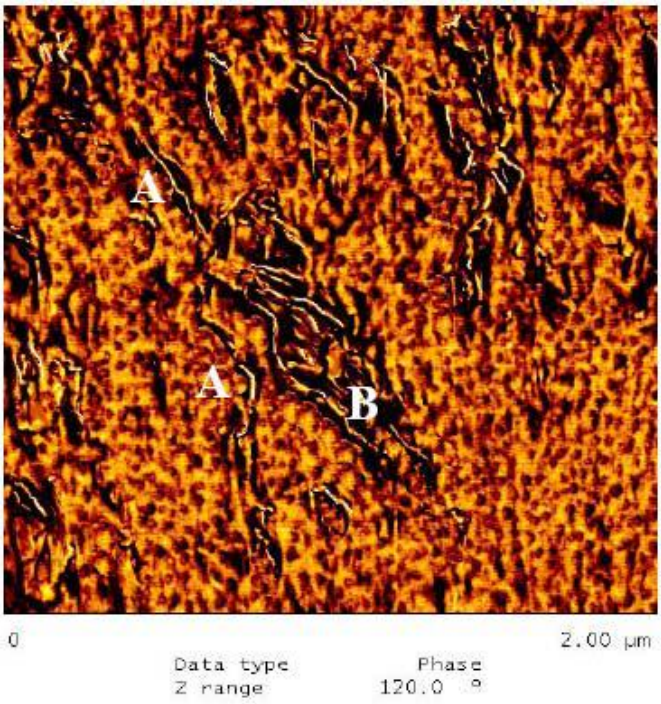

Figure 3. AFM image of PP-mPP with 7% Cloisite where: A - stacks of layers (intercalated tactoids), B-exfoliated monolayers

Thermo-Oxidative Degradation Study

TG analysis of PP and PP nanocomposite (PP-MAPP-Cloisite 20A) show that at heating in air at 10°C/min, PP volatilizes completely, in two steps beginning at about 300°C with maximum rate at 400°C through a radical chain process propagated by carbon centered radicals originated by carbon-carbon bond scission (Fig.4) [12]. Below 200°C, the hydroperoxidation on C-H bonds, in which oxygen addition occurs to the carbon radicals created within the polymer chain by H abstraction initiates radical-chain degradation of PP [13], whereas above 200-250°C, oxidative dehydrogenation of PP takes over [14]. Depolymerization and random scission by direct thermal clevege of carbon-carbon bonds becomes possible in air as in nitrogen, above 300°C.

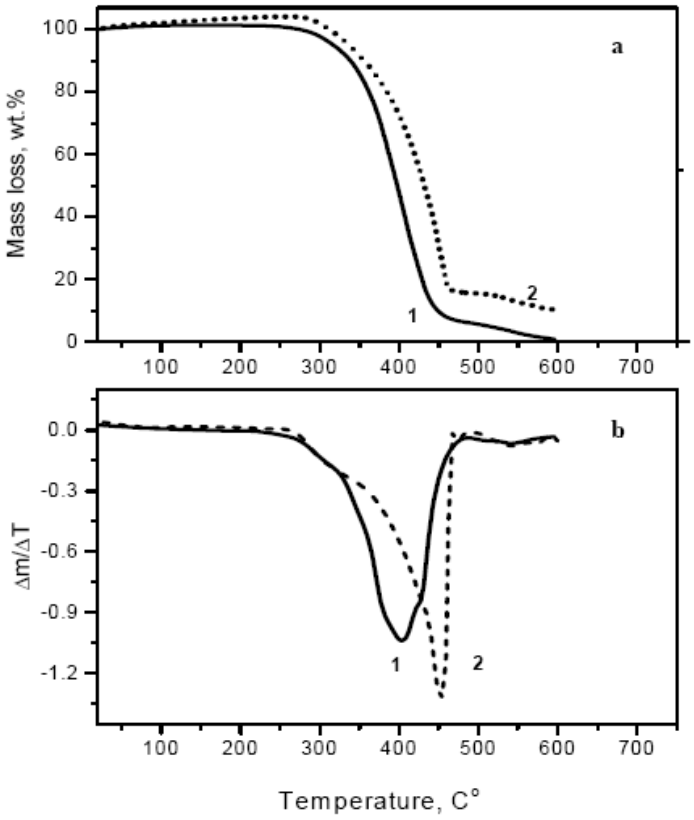

Figure 4. TG – (a) and DTG – (b) curves of PP (1) and PP-MAPP-Cloisite 20A (2) in air at the heating rate of 10K/min

Stabilizing effect of Δ50°C (Fig.4 b) of PP-MAPP-Cloisite 20A over neat PP calculated with the maximum rate of mass loss can be explain by means of the barrier effect of the silicate nanolayers which operate in the nanocomposite level against oxygen diffusion, shielding the polymer from its action.

A char residue from neat PP is left at 450°C (5%), due to charring promoted by oxidative dehydrogenation. Then it slowly decomposes on heating up to 600°C in air (Fig.4). On the other hand, thermal degradation of PP-MAPP-Cloisite 20A in air results to much more stable char form which doesn't oxidize even at 600^{o}C (Fig. 4 and 5).

Silicate nanostructure executes a role of efficient barrier to oxygen diffusion towards the native polymer. Surface polymer molecules trapped within the silicate are thus brought to a close contact with oxygen and catalytic - silicate layers to produce the thermally and oxidative steady carbonized structures (Scheme on Fig.5).

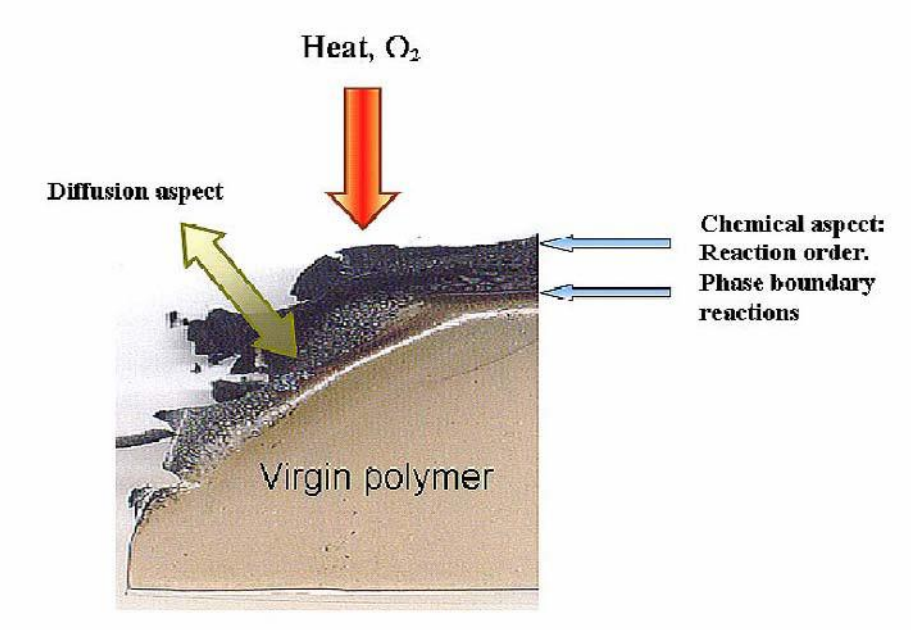

Figure 5. Scheme of the thermo-oxidative degradation of PP nanocomposite (PP-MAPP-Cloisite 20A)

Kinetic Analysis Using TGA Data

Kinetic studies of materials degradation have been carried out for many years using numerous techniques to analyze the data. Most often, TGA is the experimental method of choice and the only technique to be explored here. TGA involves placing a sample of polymer on a microbalance within a furnace and monitoring the weight of the sample during some temperature program. It is generally accepted that materials degradation obeys the basic equation (1) [15]

$$dc/dt = - F(t,T\ c_o\ c_f) \quad (1)$$

where: t - time, T - temperature, c_o - initial concentration of the reactant, and c_f - concentration of the final product. Equation $F(t,T,c_o,c_f)$ can be described by two separable functions, $k(T)$ and $f(c_o,c_f)$:

$$F(t,T,c_o,c_f) = k(T(t)\cdot f(c_o,c_f) \quad (2)$$

Arrhenius equation (4) will be assumed to be valid for the following:

$$k(T) = A\cdot\exp(-E/RT) \quad (3)$$

Therefore,

$$dc/dt= - A\cdot\exp(-E/RT)\cdot f(c_o,c_f\ ) \quad (4)$$

A series of reactions types: classic homogeneous reactions and typical solid state reactions, is listed in Table 1 [15].

Table 1. Reaction types and corresponding reaction equations,
dc/dt= - A·exp(-E/RT)·f(c_o,c_f)

Name	$f(c_o,c_f)$	Reaction type
F_1	c	first-order reaction
F_2	c^2	second-order reaction
F_n	c^n	n^{th}-order reaction
R_2	$2 \cdot c^{1/2}$	two-dimensional phase boundary reaction
R_3	$3 \cdot c^{2/3}$	three-dimensional phase boundary reaction
D_1	$0.5/(1 - c)$	one-dimensional diffusion
D_2	$-1/ln(c)$	two-dimensional diffusion
D_3	$1.5 \cdot e^{1/3}(c^{-1/3} - 1)$	three-dimensional diffusion (Jander's type)
D_4	$1.5/(c^{-1/3} - 1)$	three-dimensional diffusion (Ginstling-Brounstein type)
B_1	$c_o \cdot c_f$	simple Prout-Tompkins equation
B_{na}	$c_o^n \cdot c_f^a$	expanded Prout-Tompkins equation (na)
C_{1-X}	$c \cdot (1+K_{cat} \cdot X)$	first-order reaction with autocatalysis through the reactants, X. $X = c_f$.
C_{n-X}	$c^n \cdot (1+K_{cat} \cdot X)$	n^{th}-order reaction with autocatalysis through the reactants, X
A_2	$2 \cdot c \cdot (-ln(c))^{1/2}$	two-dimensional nucleation
A_3	$3 \cdot c \cdot (-ln(c))^{2/3}$	three-dimensional nucleation
A_n	$N \cdot c \cdot (-ln(c))^{(n-1)/n}$	n-dimensional nucleation/nucleus growth according to Avrami/Erofeev

The analytical output must fit of measurements with different temperature profiles by means of a common kinetic model.

Kinetic analysis of PP compositions thermo-oxidative degradation at heating rates of 3, 5 and 10K/min. was carried out using NETZSCH Thermokinetics software in order to provide an extra evidence of the diffusion-stabilizing effect of nanoclay structure.

Model-free methods evaluations were chosen as the starting points in kinetic analysis of neat PP and PP-mPP with 7% Cloisite 20A for determining the activation energy in the development of the model. Figure 6 shows a corresponding Friedman analysis, where the activation energy is a function of partial mass loss change [16].

The curves show higher values at the beginning of the sintering process, i.e. at lower partial-length-change values, and considerably higher values at the end of the process (a) and particularly (b). This indicates the presence of a multiple-step process.

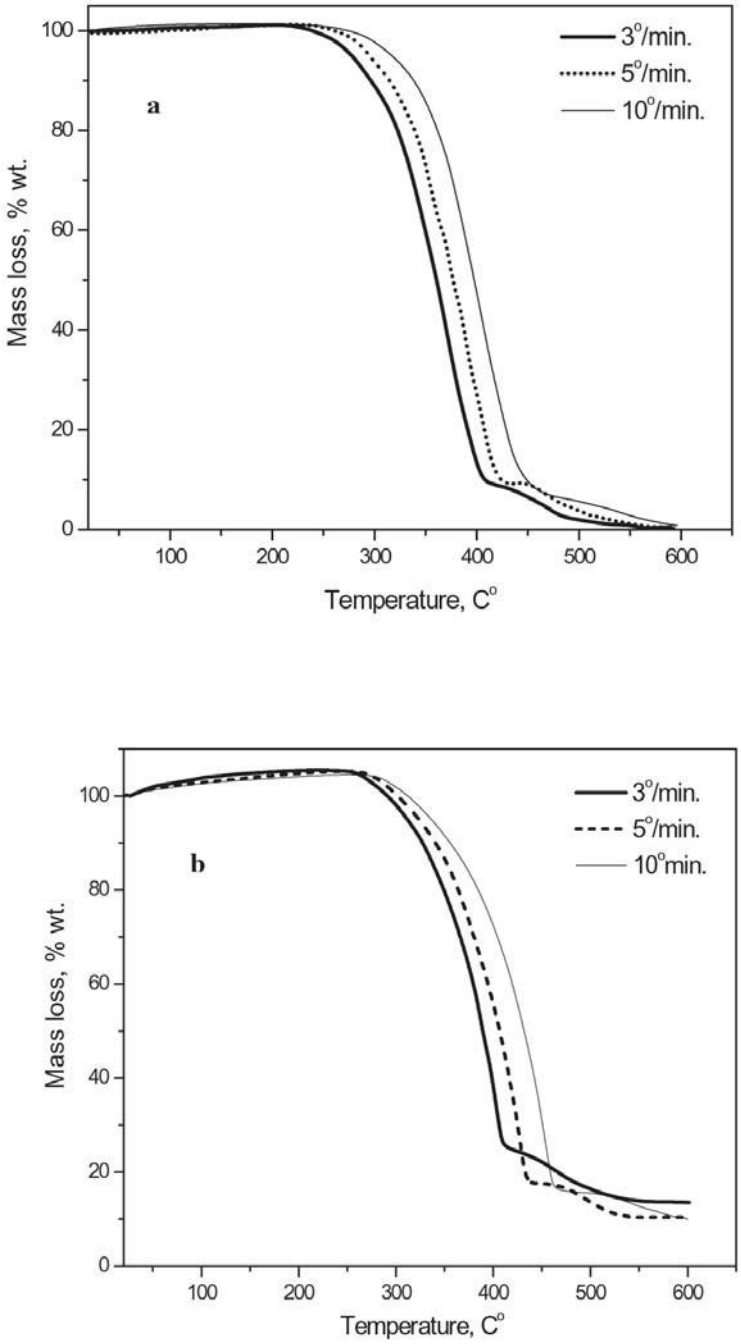

Figure 6. Friedman Analysis of neat PP – (a) and PP-MAPP-Cloisite 20A – (b)

First round analysis by Friedman method indicates a complexity of the scheme for neat PP and PP-MAPP-Cloisite 20A thermal degradation in air [16]. Nonlinear fitting procedure established the two - stage scheme for neat PP

$$A \rightarrow X_1 \rightarrow B \rightarrow X_2 \rightarrow C \quad (4)$$

and the triple - stage scheme for PP-mPP with 7% Cloisite 20A (Fig. 4 a, b) [15,17].

$$A \rightarrow X_1 \rightarrow B \rightarrow X_2 \rightarrow C \rightarrow X_3 \rightarrow D \quad (5)$$

Taking these findings into consideration for neat PP, a fit was attempted using nonlinear regression with model (4), where the nth-order (F_n) reaction type was used for all steps of the reaction (Fig. 7, Table 2).

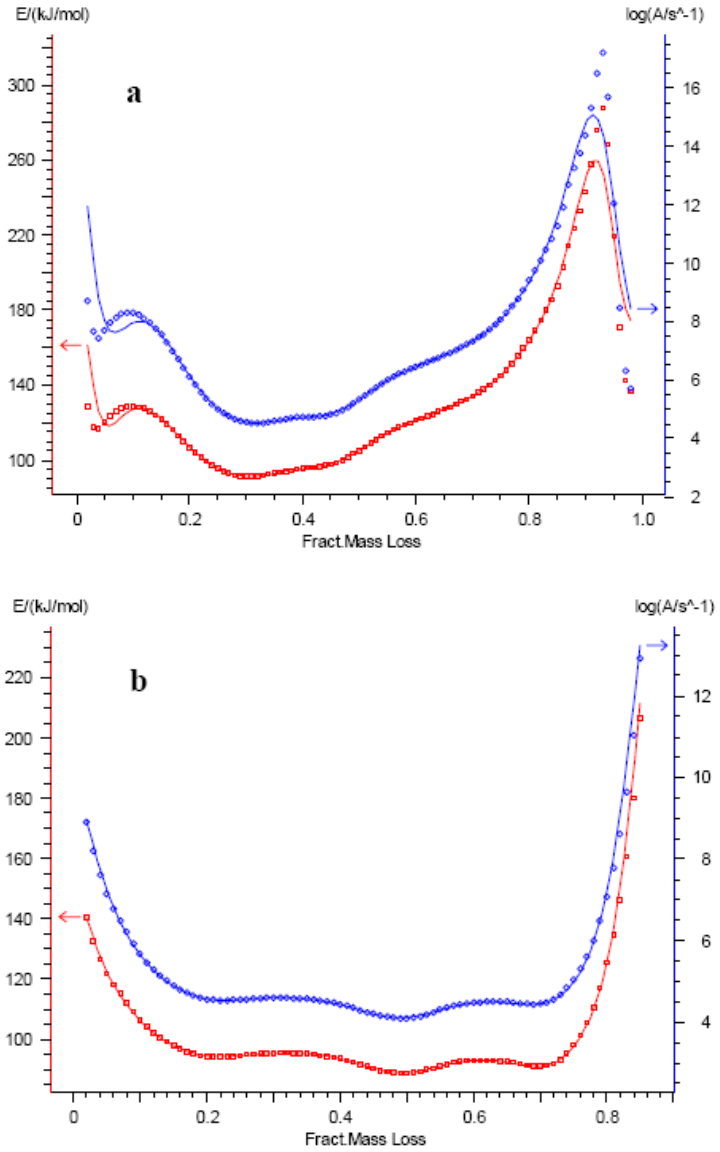

Figure 7. Nonlinear kinetic modelling for neat PP. Comparison between experimental TG data (dots) and model results (lines) at the heating rates of 3, 5 and 10K/min

With this expanded model, an excellent fit is possible for all three measurements. The kinetic parameters are listed in Table 2.

Table 2. Kinetic parameters resulting from multiple-curve analyses (heating rates 3, 5 and 10 K/min) with reaction model (A→X_1→B →X_2→C) from TG measurement of neat PP

Reaction models (types, X*i*)	Parameter	Value	Corr. Coeff.
$F_n \rightarrow F_n$	$\log A_1$, s^{-1} E_1, kJ/mol n_1	6.4 110.3 1.13	0.9994
	$\log A_2$, s^{-1} E_2, kJ/mol n_2	9.9 151.6 2.59	

A more sophisticated model (5), based on different reaction types, was chosen for PP-MAPP-Cloisite 20A thermo-oxidative degradation. The parameters are listed in Table 3.

Table 3. Kinetic parameters resulting from multiple-curve analyses (heating rates 3, 5 and 10 K/min) with different reaction models (A→X_1→B →X_2→C→X_3→D) from TG measurement of PP-MAPP-Cloisite 20A

Reaction models (types, X*i*)	Parameter	Value	Corr. Coeff.
$F_n \rightarrow F_n \rightarrow F_n$	$\log A_1$, s^{-1} E_1, kJ/mol n_1	6.3 113.4 1.16	0.9974
	$\log A_2$, s^{-1} E_2, kJ/mol n_2	8.8 150.9 2.46	
	$\log A_3$, s^{-1} E_3, kJ/mol n_3	11.5 188.5 0.78	
$F_n \rightarrow D_1 \rightarrow F_n$	$\log A_1$, s^{-1} E_1, kJ/mol n_1	6.9 113.4 1.21	0.9988
	$\log A_2$, s^{-1} E_2, kJ/mol	4.7 100.0	
	$\log A_3$, s^{-1} E_3, kJ/mol n_3	12.0 199.8 1.17	

Table 3. Continued

Reaction models (types, X*i*)	Parameter	Value	Corr. Coeff.
$F_n \rightarrow D_2 \rightarrow F_n$	$\log A_1$, s^{-1} E_1, kJ/mol n_1	6.4 113.3 1.68	0.9974
	$\log A_2$, s^{-1} E_2, kJ/mol	6.2 118.4	
	$\log A_3$, s^{-1} E_3, kJ/mol n_3	11.7 197.2 0.95	
$F_n \rightarrow D_3 \rightarrow F_n$	$\log A_1$, s^{-1} E_1, kJ/mol n_1	6.5 113.6 2.04	0.9973
	$\log A_2$, s^{-1} E_2, kJ/mol	8.3 152.3	
	$\log A_3$, s^{-1} E_3, kJ/mol n_3	11.8 197.1 0.94	
$F_n \rightarrow D_4 \rightarrow F_n$	$\log A_1$, s^{-1} E_1, kJ/mol n_1	6.6 113.7 2.01	0.9973
	$\log A_2$, s^{-1} E_2, kJ/mol	7.2 138.9	
	$\log A_3$, s^{-1} E_3, kJ/mol n_3	11.9 195.2 0.98	
$F_n \rightarrow A_2 \rightarrow F_n$	$\log A_1$, s^{-1} E_1, kJ/mol n_1	6.6 114.4 2.10	0.9975
	$\log A_2$, s^{-1} E_2, kJ/mol	5.6 105.2	
	$\log A_3$, s^{-1} E_3, kJ/mol n_3	12.0 199.3 1.23	
$F_n \rightarrow A_3 \rightarrow F_n$	$\log A_1$, s^{-1} E_1, kJ/mol n_1	6.5 114.1 2.02	0.9976
	$\log A_2$, s^{-1} E_2, kJ/mol	4.8 95.3	
	$\log A_3$, s^{-1} E_3, kJ/mol n_3	12.4 200.1 1.46	

Table 3. Continued

Reaction models (types, X*i*)	Parameter	Value	Corr. Coeff.
$F_n \rightarrow A_n \rightarrow F_n$	$\log A_1$, s^{-1} E_1, kJ/mol n_1	6.7 114.7 0.97	0.9983
	$\log A_2$, s^{-1} E_2, kJ/mol	4.7 97.7	
	$\log A_3$, s^{-1} E_3, kJ/mol n_3	11.9 200.0 1.26	
$F_n \rightarrow R_2 \rightarrow F_n$	$\log A_1$, s^{-1} E_1, kJ/mol n_1	7.1 114.9 1.27	0.9979
	$\log A_2$, s^{-1} E_2, kJ/mol	5.1 105.7	
	$\log A_3$, s^{-1} E_3, kJ/mol n_3	12.1 200.3 1.76	
$F_n \rightarrow R_3 \rightarrow F_n$	$\log A_1$, s^{-1} E_1, kJ/mol n_1	7.2 114.6 1.10	0.9978
	$\log A_2$, s^{-1} E_2, kJ/mol	5.2 108.9	
	$\log A_3$, s^{-1} E_3, kJ/mol n_3	11.6 188.5 0.78	

Taking these fittings for PP-MAPP-Cloisite 20A, a best approximation was attempted using nonlinear regression with model (5), based on the best fit quality (correlation coefficient) (Fig. 8), where the one-dimensional diffusion (D_1) reaction type was used for the second step of the reaction (Table 3), whereas the n^{th}-order reaction models were chosen for the first and third steps respectively.

These results show that the second step in thermo-oxidative degradation of PP-MAPP-Cloisite 20A is described by one-dimensional diffusion (D_1) reaction type which is liable for the overall process of the carbonization in nanocomposite polypropylene structure.

Flame Resistant Properties

The recent interest in the reported char-promoting functionalized dispersed nanoclays to yield nanocomposite structures having enhanced fire and mechanical properties, when the clays are present only at levels of 2~10%, prompts their investigation as potential fire retardants. Because of its wholly aliphatic hydrocarbon structure, neat polypropylene by itself burns very rapidly with a relatively smoke-free flame and without leaving a char residue. It

has a high self-ignition temperature (570°C), a rapid decomposition rates and hence has a high flammability.

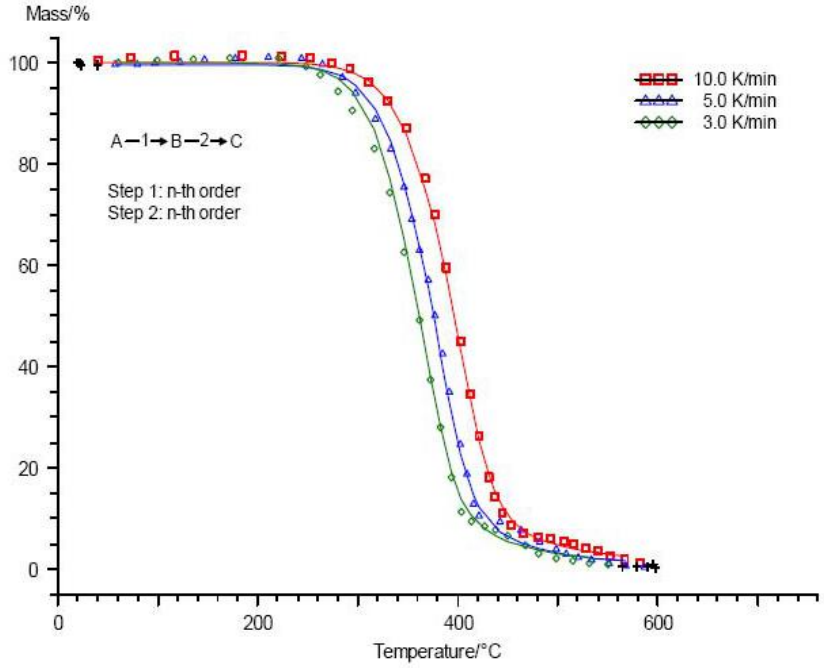

Figure 8. Nonlinear kinetic modelling for PP-MAPP-Cloisite 20A. Comparison between experimental TG data (dots) and model results (lines) at the heating rates of 3, 5 and 10K/min

Polypropylene nanocomposites have attracted more and more interest in flame retardant area in recent years due to their improved fire properties [18-20]. It is suggested that the presence of clay can enhance the char formation providing a transient protective barrier and hence slowing down the degradation of the matrix [19, 20].

The kinetic results of the present study let us the starting point to predict the mass loss of material under isothermal pyrolysis conditions using the same thermokinetics software. Figure 9 shows the fractional mass loss curves as a function of time with temperature (400 – 600^{o}C) as a parameter.

It is clearly seen that under conditions of polymer ignition and initial surface combustion, the mass loss for PP-MAPP-Cloisite 20A and its rate are noticeably lower then adequate values for the neat PP. An improvement in flame resistance of PP-MAPP-Cloisite 20A over the neat PP happens as a result of the char formation providing a transient protective barrier. In the present study this phenomena was interpreted in terms of isothermal kinetic analysis.

Apart from this information, the graphs of mass loss rates (*dm/dt*) vs. time for neat PP and PP-MAPP-Cloisite 20A indicate the depression of the degradation (fuel) products under the isothermal pyrolysis conditions at 600^{o}C (Fig. 10). It is well known that the temperature of 600^{o}C corresponds to an incident heat flux of 35 kW/m^{2}; this is referred to the real scale fire scenario [21].

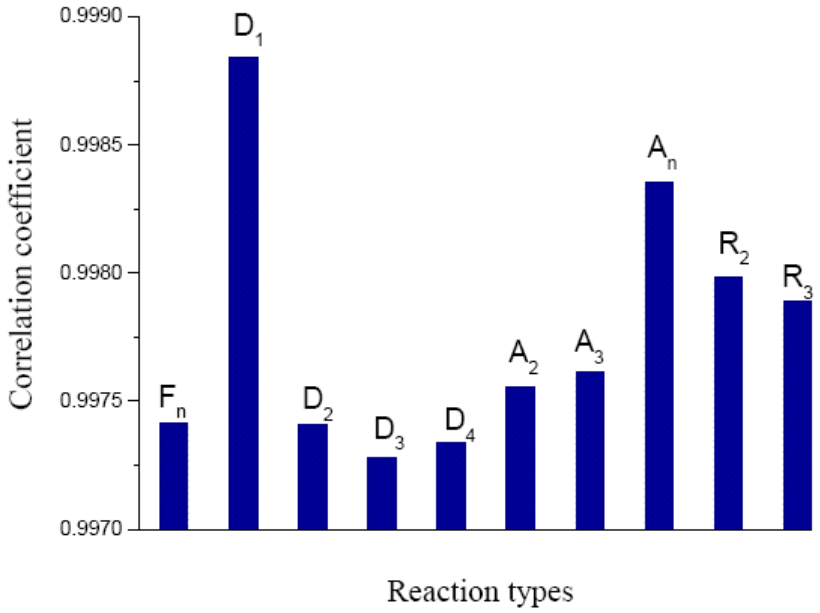

Figure 9. Fractional reaction vs. time for neat PP (a) and PP-MAPP-Cloisite 20A (b)

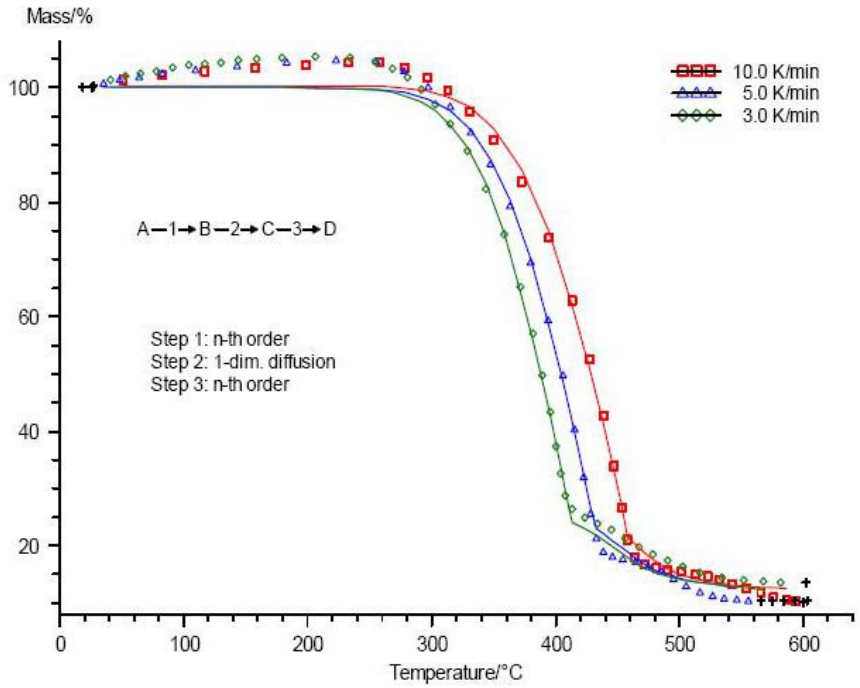

Figure 10. Mass loss rates vs. time for neat PP-MAPP-Cloisite 20A (2) under the isothermal heating condition of 600°C

The cone calorimeter is one of the most effective bench-scale methods for studying the flammability properties of materials. Fire-relevant properties, measured by the cone

calorimeter, such as heat release rate (RHR), maximum RHR, smoke and carbon monoxide yield, are vital to the evaluation of the fire safety of materials [22].

In the present study the combustibility of polypropylene nanocomposite was evaluated by a cone calorimeter. The tests were performed at an incident heat flux of 35 kW/m^2 using the cone heater [21]. Peak heat release rate (RHR), mass loss rate (MLR), specific extinction area (SEA) data, carbon monoxide and heat of combustion data measured at 35 kW/m2, are presented in Figs. 11 and 12.

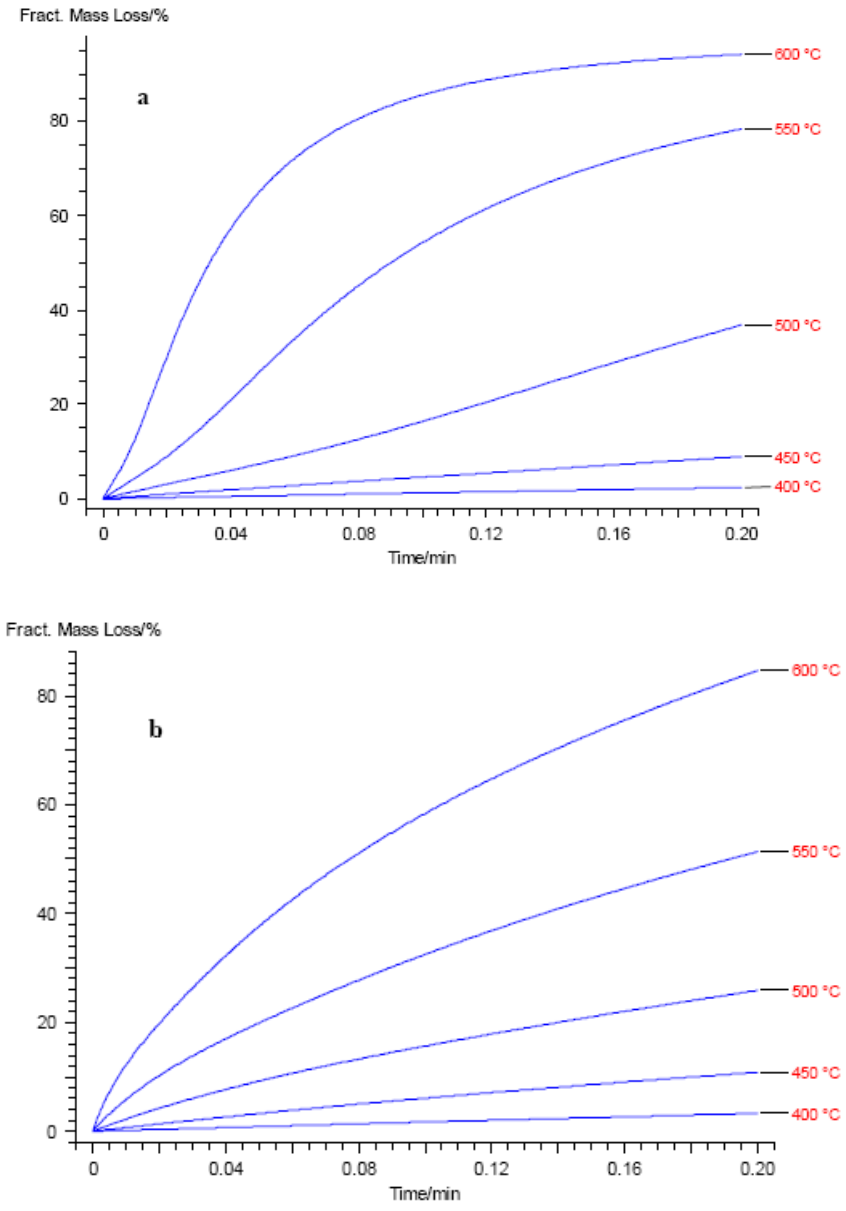

Figure 11. Rate of heat release vs. time for PP and PP-MAPP-Cloisite 20A

The RHR plots for PP-MAPP-Cloisite 20A nanocomposite and PP at 35 kW/m^2 heat flux shown in Figure indicate a 60% - decrease of peak of RHR (Fig.11). Comparison of the Cone calorimeter data PP and PP-MAPP- 7% Cloisite 20A reveals that the specific heat of combustion (H_c), specific extinction area (SEA), a measure of smoke yield, and carbon monoxide yields are practically unchanged; this suggests that the source of the improved flammability properties of these materials is due to differences in condensed-phase decomposition processes and not to a gas-phase effect. The primary parameter responsible for the lower RHR of the nanocomposites is the mass loss rate (MLR) during combustion, which is significantly reduced from the value observed for the pure PP (Fig.12). It is supposed, that this effect is caused by ability to initiate the formation of char barrier on a surface of burning polymeric nanocomposites that drastically limits the heat and mass transfer in a burning zone.

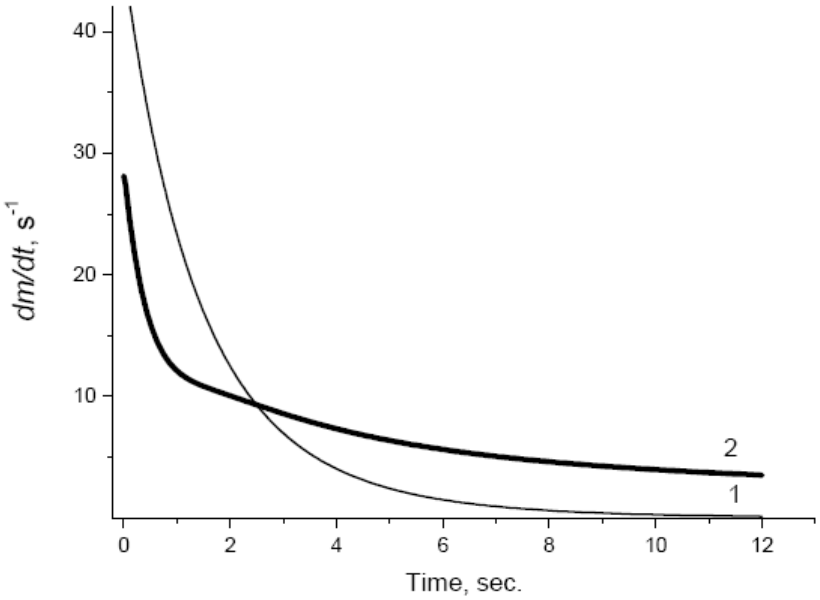

Figure 12. Mass loss rate vs. time for PP and PP-MAPP-Cloisite 20A

CONCLUSION

The kinetic data obtained by dynamic TGA designate thermal stabilization effect of nanoclay structure into a polymer matrix, caused in one-dimensional diffusion process of catalytic-charring throughout the thermal degradation of PP nanocomposition. According to provided kinetic analysis, polypropylene nanocomposite demonstrated the transcendent thermal and fireproof behaviour in relation to neat polypropylene.

Based on modern concepts of the mechanisms of polymer nanocomposites flame retardancy and char formation, it is possible to assume that simulation of dynamic behavior of anisotropic particles with the different types of morphology and relationship of geometric dimensions presented in viscous polymeric melt will be one of the promising trends in this field of research.

On the other hand, the unique barrier properties of nano-dispersed polymeric composites are of interest of polymer combustion due to specific laminar morphology. This type of structure is especially effective in comparison with the other forms of fillers because of the "labyrinth effect". Researches in this area will allow defining an influence of diffusion of low-molecular products of pyrolysis on the process of micro-intumescence in a superficial layer of burning polymers.

ACKNOWLEDGEMENTS

This work was supported by the Russian Foundation for Basic Research, project N 04-03-32052.

The authors are pleased to acknowledge the Moscow division of NETZSCH-Gerätebau GmbH for Thermokinetics software.

REFERENCES

[1] Bockhorn, H, A. Hornung, A, Hornung, U, Schawaller, D, *Journal of Analytical and Applied.*

[2] Pyrolysis, 48(2):93 (1999).2. Ballice, L, Reimert, R, *Chemical Engineering and Processing*, 41:289 (2002).

[3] Murty, MVS, Rangarajan, P, Grulke, EA, Bhattacharyya, D, *Fuel Processing and Technology*, 49:75 (1996).

[4] Chan, JH, Balke, ST, *Polymer Degradation and Stability*, Volume 57:135 (1997).

[5] Gao, Z, Kaneko, T, Amasak,i I, Nakada, M, *Polymer Degradation and Stability*, 80:269 (2003).

[6] Giannelis, E, *Adv Mater*, 8:29 (1996).

[7] Gilman, JW., Kashiwagi, T, Nyden, MR, Brown, JET, Jackson, C L, Lomakin, SM, Giannelis, E P, Manias, E, in *Chemistry and Technology of Polymer Additives*, Chapter 14, ed by Ak-Malaika S, Golovoy A, Wilkie CA, p 249, Blackwell Science Inc., Malden MA (1999).

[8] Zanetti, M, Lomakin, S, Camino, G, *Macromol Mater Eng*, 279:1-9 (2000).

[9] Kojima, Y., Usuki, A., Kawasumi, M., Okada, A., Fukushima, Y., Kurauch,i T., Kamigaito O., *J Mater Res*, 8:1185 (1993).

[10] Zanetti, M, Camino, G, Reichert, P, Mülhaupt, R, *Macromolecular Rapid Communications* 22:176-180 (2001).

[11] Qin, H, Zhang, S, Zhao, C, Feng, M, Yang, M, Shu, Z, Yang, S, *Polymer Degradation and Stability*, 85:807 (2004).

[12] Grassie, N, Scott, G, in *Polymer degradation and stabilization*, Cambridge University Press, Cambridge, p 275 (1985).

[13] March, J, in *Advanced Organic Chemistry*, McGraw-Hill Kogakusa Ltd, Tokyo, p.367 (1977).

[14] Benson, SW, Nogia, PS, *Account of Chemical Research*, 12:233 (1979).

[15] Opfermann, J, *J Thermal Anal Cal*, 60: 641 (2000).

[16] Friedman, HL, *J Polym. Sci*., C6:175 (1965).
[17] Opfermann, J, Kaisersberger, E, *Thermochim Acta*, 11:167 (1992).
[18] Lomakin, SM, Zaikov, GE, in *Modern Polymer Flame Retardancy*, VSP Int. Sci. Publ. Utrecht, Boston, p. 272 (2003).
[19] Gilman, JW, *Applied Clay Sci*, 15:31 (1999).
[20] Gilman, GW, Jackson, C L., Morgan, A B, Harris, R H, Manias, E, Giannelis, E P, Wuthenow, M, Hilton, D, Phillips, S, *Chem. Mater*, 12:1866 (2000).
[21] Babrauskas, V, *Fire and Materials*, 19:243 (1995).
[22] Babrauskas, V., Peacock, R. D. *Fire Safety J.*, 18:255 (1992).

In: Polymers, Polymer Blends, Polymer Composites… ISBN 1-60021-168-2
Eds: A.K. Mikitaev, M.K. Ligidov et al., pp.59-67

Chapter 6

FUNDAMENTAL ASPECTS OF FILLING OF NANOCOMPOSITES WITH HIGH-ELASTICITY MATRIX: FRACTAL MODELS

Georgi V. Kozlov[1], Yurii G. Yanovskii[1]* and Gennadi E. Zaikov[2]
[1]Institute of Applied Mechanics of Russian Academy of Sciences, 119991,
Leninskii pr. 32 A, Moscow, Russian Federation
[2]N.M. Emanuel Institute of Biochemical Physics of Russian Academy of Sciences,
119991 Kosygin St. 4, Moscow, Russian Federation

ABSTRACT

In the present paper are considered three fundamental factors controlling filling processes of nanocomposites with high-elasticity matrix. They are: filler particles aggregation, strain localization and change of structure type from Euclidean object up to fractal. The last postulate is the most physically fundamental, since it demonstrates noncorrectness of description of structure and properties of nanocomposites with high-elasticity matrix within the framework of classical theory of entropic high-elasticity.

Keywords: Nanocomposite; high-elasticity matrix; filler; aggregation; strain localization; fractal structure.

INTRODUCTION

The practical importance and complexity of structure of polymer composites with matrix, which is in high-elasticity state, are due to a large number of works, devoted to studies of structure and properties of the mentioned composites. Lipatov [1] summarized obtained

*Correspondence to: Yurii G. Yanovskii, Institute of Applied Mechanics of Russian Academy of Sciences, Moscow, Russian Federation, Leninskii pr. 32 A, 119991. mailto: i_dolbin@mail.ru

results and came to the conclusion that the main factors of reinforcement of the considered composites are:

(1) the features of polymer chemical constitution and strong intermolecular interaction of it with filler particles surface;
(2) the formation of second structures by filler particles;
(3) reorganization at deformation of filled material molecular structure without its failure;
(4) the failure of network structure – rupture of filler – polymer bonds or molecular network transverse bonds.

Among other factors, influenced on the reinforcement, Lipatov marks form and size of filler particles, character of their distribution and aggregation and also a number of common physical-chemical causes, typical for all polymer composites [1].

DISCUSSION

Not rejecting correctness of these principles, becoming already classical, we nevertheless distinguished three fundamental factors, the role of which happens obvious owing to the fractal analysis application for the description of polymer composites structure and properties [2-4].

The first of these factors is filler particles aggregation. The detailed description of this effect influence on structure and properties of composites, having glassy matrix, is given in review [3]. For the considered composites this effect is important first of all for determination of filler volume fraction φ_f, which is calculated by division of filler mass fraction into its density. However, filler particles in real composites exist in the form of fractal aggregates, which density can be more smaller than monolithic object of such filler. Below the example of value φ_f calculation for concrete composite will be given.

The second aspect of filler particles aggregation is the possibility of taking into consideration occlusive rubber in aggregates of these particles. As it is known [5], the relationship between fractal aggregate radius R_{ag}, and particles number N in it will look like:

$$R_{ag} \sim N^{1/d_f} \tag{1}$$

where d_f is fractal dimension of filler particles aggregate.

The rise of occlusive rubber fraction in aggregate at condition R_{ag}=const means decrease N and reduction d_f. This gives the possibility of quantitative calculation of occlusive rubber fraction in aggregate.

And at last, the third important aspect of aggregation process is its mechanism. As it is known [6], within the framework of irreversible aggregation models are possible two aggregation mechanisms: cluster-cluster and particle-cluster, the physical sense of which follows from its name. Within the framework of the first mechanism the value R_{ag} is determined by the relationship [3]:

$$R_{ag} \sim \left(\frac{4c_0 kT}{3\eta m_0} \right)^{1/d_f} t^{1/d_f} \tag{2}$$

where c_0 is initial concentration of filler particles, k is Boltzmann constant, T is temperature, η is medium viscosity, m_0 is initial particle mass, t is aggregation duration.

For particle-cluster mechanism the value R_{ag} is determined like this [6]:

$$R_{ag} \sim c_0^{-1/(d-d_f)} \tag{3}$$

where d is dimension of Euclidean space, in which a fractal (obviously, in our case d=3) is considered.

From the relationship (2) follows, that at cluster-cluster aggregation (merging of small aggregates in largerones) the value R_{ag} can be controlled by variation of parameters T, η, m_0, d_f and t. But the most interesting is c_0 role, i.e., filler content, in regulation of value R_{ag}: for cluster-cluster mechanism the c_0 rise results to increase R_{ag} and for particle-cluster mechanism – to its reduction. In this aspect the most interesting is the relationship (3), since from it follows, that at definite conditions the aggregation process can be suppressed by c_0. Therefore, the ability of aggregation mechanism change is the perspective instrument of control of structure of filler particles aggregates. Besides, the value d_f ($\approx$ 2.50) for particle-cluster aggregation mechanism is essentially more than corresponding dimension ($d_f \approx$1.80-2.10 [6]) for cluster-cluster mechanism, i.e., the first of the mentioned mechanisms allows to obtain more compact aggregates, practically not containing occlusive rubber.

The second important factor is the calculation of draw ratio λ for composites. This problem is due to heterogeneity of composite structure, consisting of two phases elasticity modulus of one of them is essentially (in some orders of value) more, than the second. Differently speaking, during composite tension process only one phase is extended, namely, rubber, owing to nominal value λ not already does describe adequately composite deformation process. This effect is well known and for its quantitative accounting for there are two models. The first of them uses the equation [7]:

$$\lambda_{mol} = \frac{\lambda}{1-\varphi_f} \tag{4}$$

where λ_{mol} is molecular draw ratio.

The equation (4) recommended itself well at the description of extrudates of componors based on the ultrahighmolecular polyethylene [2]. The second model uses more precise equation for calculation of local draw ratio of two-phase polymeric material [8]:

$$\lambda = \lambda_p (1-\varphi_f) + \lambda_f \varphi_f \tag{5}$$

where λ_p and λ_f are draw ratio for polymeric matrix and filler, accordingly.

Returning to the question of filler particles aggregation, it should be noted, that for compact aggregates of high-modulus filler λ_f=1 and then from comparison of the equations (4) and (5) follows, that for large enough λ $\lambda_{mol} \approx \lambda_p$. However, this situation can be essentially changed for loose (having rather small dimension d_f) aggregates, containing of occlusiv rubber significant fraction. For them λ_f>1 can be expected, that reduces the value λ_p at λ=const, i.e., weakens reinforcing the action of the filler.

And at last, the third and the most fundamental factor is the change of nanocomposite structure at the introduction of particulate filler in high-elasticity polymeric matrix. As Balankin showed [9], classical theory of entropic high-elasticity has a number of principal deficiencies due to non-fulfilment for real rubbers of two main postulates of this theory, namely, essentially non-Gaussian statistics of real polymeric networks and lack of co-ordination of postulates about Gaussian statistics and incompressibility of elastic materials. Last postulate means, that Poisson's ratio ν of these materials must be equal to 0.5. As it is known [10], Gaussian statistics of macromolecular coil is correct only in case of its dimension D_f=2.0, i.e., for coil in θ-solvent. Since between value D_f and fractal dimension d_f^p of polymer's condensed state structure exists the relationship [11]:

$$d_f^p = 1.5 D_f \tag{6}$$

then for execution of chains Gaussian statistics condition in volume polymer the criterion d_f^p=3 realization is required, i.e., the polymer structure must be Euclidean object. If the last condition with definite provisos is carried out for nonfilled rubbers, then the introduction in rubber filler with significantly smaller Poisson's ratio ν_f will decrease the value ν of composite as system. Since the value of fractal dimension of composite structure d_f^c is determined like that [12]:

$$d_f^c = (d-1)(1+\nu) \tag{7}$$

then this means, that the classical entropic high-elasticity theory is applied only to Euclidean objects (ν=0.5, d_f^c=3.0) and, accordingly, inapplicable for description of rubbers, filled by particulate filler, of which ν<0.5 and d_f<d=3, i.e., which are fractal objects. Therefore, for description of such objects behaviour the fractal theory of elasticity and entropic high-elasticity should be used [9].

In order to demonstrate the correctness of expounded above general postulates, let's make quantitative estimations of the dependence of stress σ on φ_f and T for rubber SKI-3 filled by technical carbon P-234 according to the data of paper [13]. For this let's make approximated, by plausible assumption, that the technical carbon particles with diameter d_{part}=50 mnm [13] form the aggregates from five particles. Then the radius of such aggregate can be estimated according to the equation [14]:

$$R_{ag} = \left(\frac{n_{part} S}{\pi \eta_p} \right)^{1/2} \tag{8}$$

where n_{part} is particles number in aggregate, S is cross-sectional area of particle, η_p is packing density, which is equal to 0.74 for monodisperse circles [15].

At n_{part}=5 and d_{part}=50 mnm R_{ag}≈65 mnm. The density of such aggregate ρ_{ag} is estimated as follows [16]:

$$\rho_{ag} = \rho_{dens} \left(\frac{R_{ag}}{a} \right)^{d_f - d} \tag{9}$$

where ρ_{dens} is aggregate substance density in dense packing state (ρ_{dens}=2700 kg/m^3 for carbon [3]), a is lower boundary of aggregate fractal behaviour accepted equal to 15 mnm [17]. For d_f=2.5, d=3 ρ_{ag}≈1300 kg/m^3 will be obtained, that is more than two times smaller than density of filler mass content into value ρ_{ag} and calculate molecular (real) draw ratio $\lambda_{mol}=\lambda_p$ of polymeric matrix according to the equation (5). Estimating shear modulus G according to the known equations of high-elasticity classical theory [18], let's calculate Poisson's ratio according to the equation [19]:

$$\nu = \nu_r \left(1 - \varphi_f \right) + \varphi_f \nu_f \tag{10}$$

where ν_r and ν_f are values of Poisson's ratio for rubber and filler, accepted equal to 0.50 and 0.25, accordingly.

Further the main equation of high-elasticity fractal theory for σ calculation in its simplified form will be used [9]:

$$\sigma = \frac{E}{1 + 2\nu + 4\nu^3} \left[\lambda_{mol}^{1+2\nu} - 2\nu \lambda_{mol}^{-1-2\nu(1+\nu)} - (1 - 2\nu) \lambda_{mol}^{-2\nu} \right] \tag{11}$$

where elasticity modulus is defined this way [20]:

$$E = 2(1 + \nu) G \tag{12}$$

As follows from the data of Fig. 1, where the comparison of experimental σ^e is made and calculated according to the considered above method σ^T stress of SKI-3 and based on it composites with technical carbon content 20, 30, 40 and 60 mass. % at two testing temperatures (250 and 380 K), good enough correspondence of theory and experiment is obtained, despite arbitrary choice of important parameters number. Two interesting moments should be noted. Firstly, for nonfilled rubber SKI-3 the calculation is made at ν=0.5. Secondly, from the plot of Fig 1 follows, that at small φ_f the values σ^T are somewhat more σ^e and at large φ_f the relation is opposite. This observation can assume an aggregation

amplification at filler's content increase, i.e., the R_{ag} rise or aggregates compactness reduction, i.e., d_f decrease.

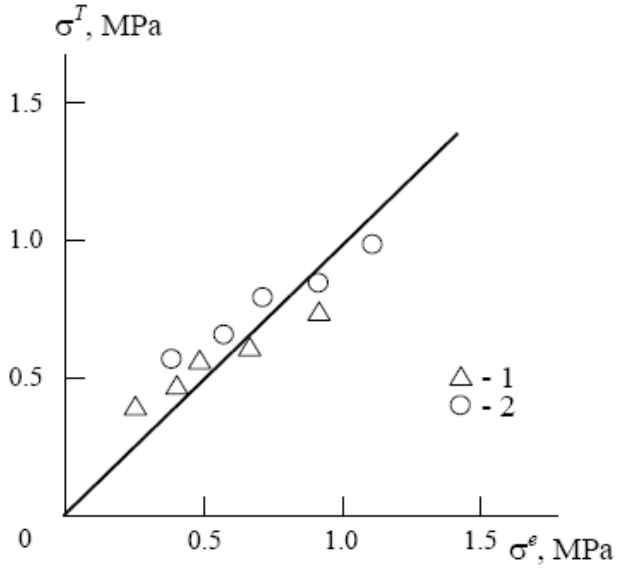

Figure 1. The comparison of experimental σ^e and calculated according to the equation (11) σ^T stress values at temperatures 250 (1) and 380 K (2) for rubber SKI-3, filled by technical carbon

As it is known [18], within the framework of high-elasticity classical theory the value σ is described with the aid of the two following equations:

$$\sigma = G\left(\lambda^2 - \lambda^{-1}\right) \tag{13}$$

$$\sigma = A\left(\lambda - \lambda^{-1/2}\right) \tag{14}$$

where A is material constant.

In Fig. 2 and 3 the dependences σ on generalized stress for studied rubbers, corresponding to the equations (13) and (14), are shown. As can be seen, in case of composites the linearity of these dependences is violated, i.e., at least, the filled rubbers behaviour does not corresponded to high-elasticity classical theory, that is assumed above. Differently speaking, filled rubbers are impossible to consider as ideal, for which internal energy change ΔU is equal to zero in deformation process.

Within the framework of high-elasticity theory the value G in the equation (13) is determined as follows [18]:

$$G = NkT \tag{15}$$

where N is active chains number on rubber volume unit.

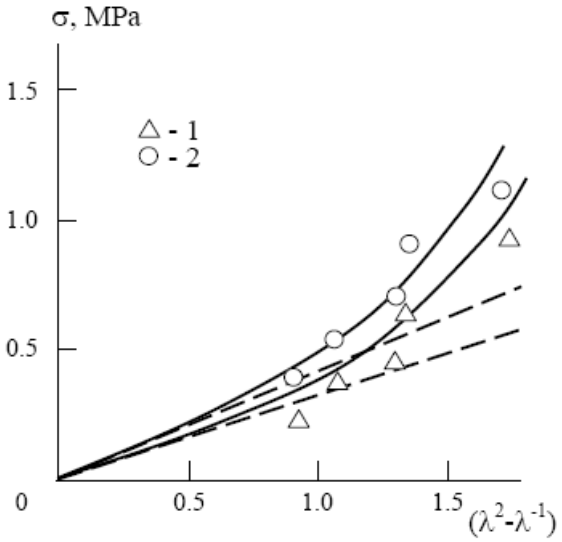

Figure 2. The dependence of stress σ on generalized strain $(\lambda^2-\lambda^{-1})$ at temperatures 250 (1) and 380 K (2) for rubber SKI-3, filled by technical carbon. The shaded lines are shown the dependencies assumed by high-elasticity classical theory

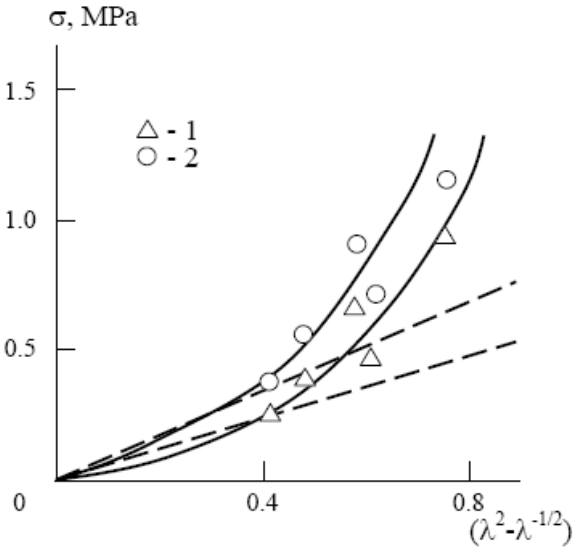

Figure 3. The dependence of stress σ on generalized strain $(\lambda-\lambda^{-1/2})$ at temperatures 250 (1) and 380 K (2) for rubber SKI-3, filled by technical carbon. The shaded lines are shown the dependencies assumed by high-elasticity classical theory

From combination of the equations (13) and (15) follows, that at T=0 K G=0 and σ=0. However, as it is shown in paper [13], it is true only for nonfilled SKI-3, but for filled samples the linear dependence σ(T) at T=0 K is extrapolated to nonzero value $\sigma(\sigma_0)$, which is raised at φ_f increase. Besides, from the data of Fig. 2 the deviation value of the dependence $\sigma(\lambda^2-\lambda^{-1})$ Δσ from its linear extrapolation (it is shown in Fig. 2 by shaded line) can be estimated, which is supposed according to the high-elasticity classical theory (see the

equation (13)). In a Fig. 4 and 5 the dependences σ_0 and $\Delta\sigma$ on φ_f and $(d\text{-}d_f)$, accordingly are given (for convenience they were linearized by using quadratic form of dependence). As can be seen, in both cases linear correlation passing thourgh coordinates origin for $\varphi_f=0$ and $d_f=d$ is obtained, i.e., for nonfilled rubber, which is Euclidean object.

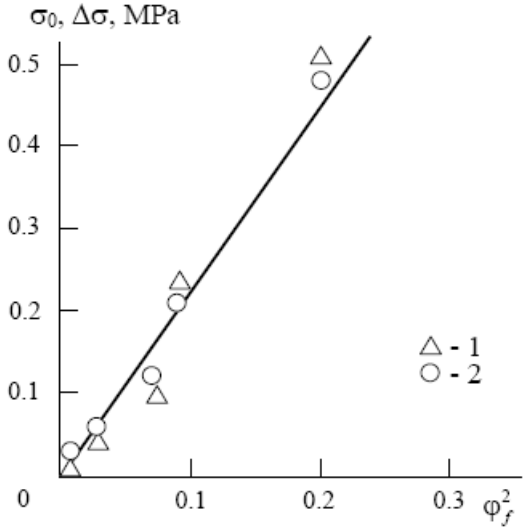

Figure 4. The dependence of deviations from high-elasticity classical theory σ_0 (1) and $\Delta\sigma$ (2) (the explanations give in the text) on filler volumetric degree φ_f for rubber SKI-3, filled by technical carbon

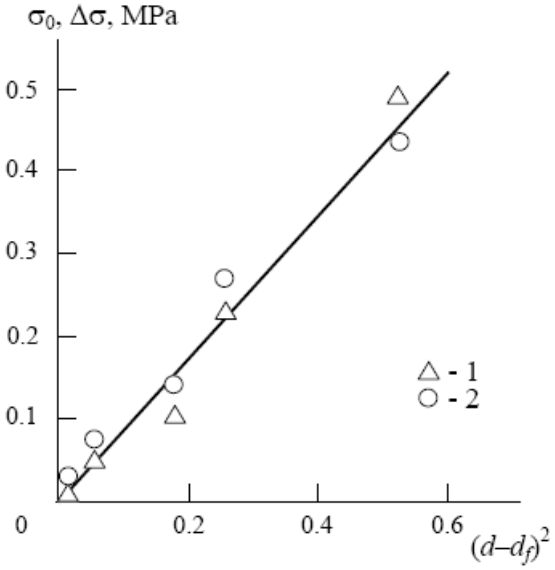

Figure 5. The dependence of deviations from high-elasticity classical theory σ_0 (1) and $\Delta\sigma$ (2) (the explanations give in the text) on Euclidean and fractal dimensions difference $(d–d_f)$ for rubber SKI-3, filled by technical carbon

CONCLUSION

Therefore, in the present paper three fundamental factors controlling filling processes of nanocomposites with high-elasticity matrix are considered. They are: filler particles aggregation, strain localization and change of structure type from Euclidean object up to fractal. The last postulate is the most physically fundamental, since it demonstrates noncorrectness of description of structure and properties of nanocomposites with high-elasticity matrix within the framework of classical theory of entropic high-elasticity.

REFERENCES

[1] Lipatov, Yu.S. *in Kompozitsionnye Polimernye Materialy*. Kiev, Naukova Dumka, p. 75 (1975).

[2] Aloev, V.Z., Kozlov, G.V., *Physics of Orientational Phenomenas in Polymeric Materials*. Nal'chik, Polygraphservis and T, 2002, 288 p.

[3] Kozlov, G.V., Yanovskii, Yu.G., Lipatov, Yu.S., *Mekhanika Kompozitsionnych Materialov i Konstruktsii*, 9: 398 (2003).

[4] Kozlov, G.V., Lipatov, Yu.S., *Poverchnost'*, 8: 81 (2003).

[5] Feder, F., *Fractaly*. Moscow, Mir, 1991, 256 p.

[6] Shogenov, V.N., Kozlov, G.V., *Fraktal'nye Klastery v Fiziko-Khimii Polimerov*. Nal'chik, Polygraphservis and T, 2002, 268 p.

[7] Watts, M.P.C., Zachariades, A.E., Porter, P.S., *J. Mater. Sci.*, 15: 426 (1980).

[8] Castellani, L., Maestrini, C., *Polymer*, 31: 2278 (1990).

[9] Balankin, A.S., *Pis'ma v ZhTF*, 17: 68 (1991).

[10] Kozlov, G.V., Zaikov, G.E., *Structure of the Polymer Amorphous State*. Utrecht-Boston, Brill Academic Publisher, 2004, 465 p.

[11] Kozlov, G.V., Temiraev, K.B., Shustov, G.B., Mashukov, N.I., *J. Appl. Polymer Sci.*, 85: 1137 (2002).

[12] Balankin, A.S., *Synergetics of Deformable Body*. Moscow, Publisher of Ministry for Defence SSSR, 1991, 404 p.

[13] Yanovskii, Yu.G., Zgaevskii, V.E., *Fizicheskaya Mezomekhanika*, 4: 63 (2001).

[14] Kozlov, G.V., Shogenov, V.N., Mikitaev, A.K., *Inzhenerno-Fizicheskii Zhurnal*, 71: 1012 (1998).

[15] Bobryshev, A.N., Kozomasov, V.N., Babin, L.O., Solomatov, V.I., *Sinergetika Kompozitsionnych Materialov*. Lipetsk, NPO ORIUS, 1994, 154 p.

[16] Brady, R.M., Ball, R.C., *Nature*, 309: 225 (1984).

[17] Avnir, D., Farin, D., Pfeifer, P., *Nature*, 308: 261 (1984).

[18] Bartenev, G.M., Frenkel, S.Ya., *Fizika Polimerov*. Leningrad, Khimiya, 1990, 432 p.

[19] Shustov, G.B., Afaunova, Z.I., Kozlov, G.V., *Vestnik KBGU. Khimicheskie nauki*, 3: 45 (1990).

[20] Kozlov, G.V., Sanditov, D.S., *Anharmonic Effects and Physical-mechanical Properties of polymers.* Novosibirsk, Nauka, 1994, 261 p.